The Journal of Chemical Physics

Development of a solvent-polarizable three-dimensional reference interaction-site model theory

Cite as: J. Chem. Phys. **152**, 114108 (2020); https://doi.org/10.1063/5.0004173
Submitted: 09 February 2020 . Accepted: 04 March 2020 . Published Online: 17 March 2020

Norio Yoshida, and Tsuyoshi Yamaguchi

The Journal of Chemical Physics ARTICLE scitation.org/journal/jcp

Development of a solvent-polarizable three-dimensional reference interaction-site model theory

Cite as: J. Chem. Phys. 152, 114108 (2020); doi: 10.1063/5.0004173
Submitted: 9 February 2020 • Accepted: 4 March 2020 •
Published Online: 17 March 2020

Norio Yoshida[1,a)] and Tsuyoshi Yamaguchi[2,a)]

AFFILIATIONS

[1] Department of Chemistry, Graduate School of Science, Kyushu University, 744 Motooka, Nishiku, Fukuoka 819-0395, Japan
[2] Graduate School of Engineering, Nagoya University, Chikusa, Nagoya 464–8603, Japan

[a)] **Authors to whom correspondence should be addressed:** noriwo@chem.kyushu-univ.jp and yamaguchi.tsuyoshi@material.nagoya-u.ac.jp

ABSTRACT

Solvent polarization around a polar solute molecule plays an essential role in determining the electronic and thermodynamic properties of solutions. In this study, a solvent-polarizable model in response to solute polarization is proposed, which is coupled with a three-dimensional reference interaction-site model theory. The charge-response kernel is used to describe solvent polarizability, and four different coupling schemes are assessed. The most feasible behavior scheme among them is the one that incorporates responses not only to solute polarization but also to solute-induced solvent polarization. The numerical results indicated that solvent molecules near the polar solute show significant polarization, and therefore, the model proposed here is useful for considering the solvation process and thermodynamics of polar solute molecules.

I. INTRODUCTION

A solvent molecule is polarized on solvating an ionic or polar solute molecule by the solute itself as well as by other solvent molecules. Such a polarization enhances the electrostatic interaction with the surroundings and plays an important role in determining the electronic and thermodynamic properties of the solution.[1] The electron transfer reaction is a typical process affected by solvent polarization. There are two major components of solvent polarization, namely, the fast electronic polarization and the relatively slow molecular orientational polarization, and they behave differently in the electron transfer reaction. When the electronic distribution of a solute molecule changes suddenly due to electron transfer, the electronic polarization immediately responds to the change, followed by the slow relaxation of the orientational polarization of the solvent molecules. The orientational polarization usually dominates the electronic polarization in the equilibrium state, but the latter polarization mainly affects the energy change for some nonequilibrium states, such as the Frank–Condon state, which are essential to the electron transfer reaction in solution.

Many polarizable models for solvent molecules have been developed.[2–9] The charge-response kernel (CRK) method developed by Morita and Kato is one of the successful models of polarizable solvents that has been applied in molecular dynamics (MD) simulation studies to various chemical and physical processes in bulk solution and at the liquid–vapor interface.[10–17] The CRK represents the response of point charges on atoms to the electrostatic potential acting on each atomic site or atomic group; the principles of CRK will be presented in Sec. II.

The method combining CRK with the reference interaction-site model (RISM) theory, a statistical mechanics theory of molecular liquids, has been proposed by Naka *et al.*[18] The RISM theory allows us to obtain the solvation structure of molecular liquids, considering the microscopic intermolecular interaction in the thermodynamic limit, unlike other popular solvation models, such as MD simulation or the continuum model.[19–21] This method was applied to evaluate the excitation energies of small organic molecules in several solvent systems, and the effect on the spectral shift of the solute molecules induced by the electronic polarization of the solvent was analyzed.[18]

To consider the solvent electronic polarization, the electrostatic potential acting on the solvent molecule generated by both the solute and other solvent molecules should be considered. However, only the effects of the solute electrostatic potential on the solvent polarization were included in the former theory for the solute–solvent systems. Thus, for further improvement, it is desirable to develop a theory that can consider the electrostatic potential from the other solvent molecules.

In the present study, we propose a solvation theory combined with a solvent-polarizable model in response to the solute polarization based on the three-dimensional (3D) RISM theory and CRK method. The 3D-RISM theory is an advanced theory of RISM suitable for describing the solvation structure and thermodynamics of fully anisotropic systems.[22–26] An advantage of using 3D-RISM is that it can handle not only complex solute molecules but also the contribution from anisotropic solvent distribution. We refer to the 3D-RISM taking solvent polarization into account with the CRK as the sp-3D-RISM theory. In this paper, we propose four different scheme types for the electrostatic potential that induces the solvent polarization. Because the induced polarized solvent charges affect the dielectric properties of the solvent on solvation, we assess the dielectric constant and refractive index. We also propose a free energy functional formalization of the sp-3D-RISM theory and an analytical expression for the solvation free energy. We applied the sp-3D-RISM theory for the hydration of monatomic ions and polar polyatomic molecules to demonstrate the advantages of the theory.

II. THEORY

A. CRK

In the present study, we employed the CRK model to take the charge polarization of the solvent molecule into account.[5,10] In this model, the partial charge on atom ν, located at position $\boldsymbol{r}$, deviates from its value in vacuum, Q_ν^{vac}, due to the electronic polarization, as

$$Q_\nu(\boldsymbol{r}) = Q_\nu^{\mathrm{vac}} + \Delta Q_\nu(\boldsymbol{r}). \tag{1}$$

The charge polarization of atom ν at position $\boldsymbol{r}$, $\Delta Q_\nu(\boldsymbol{r})$, is given as the linear response to the electronic potential on other intramolecular sites by

$$\Delta Q_\nu(\boldsymbol{r}) = \sum_{\nu'} K_{\nu\nu'} V(\boldsymbol{r} + \boldsymbol{l}_{\nu\nu'}), \tag{2}$$

where $K_{\nu\nu'}$ is a CRK and $V(\boldsymbol{r})$ is the electrostatic potential at the position $\boldsymbol{r}$. $\boldsymbol{l}_{\nu\nu'}$ is a vector connecting atoms ν and ν'. The CRK is defined as

$$K_{\nu\nu'} = \frac{\partial Q_\nu}{\partial V_{\nu'}} = \frac{\partial Q_{\nu'}}{\partial V_\nu}, \tag{3}$$

where Q_ν is the partial charge of atom ν and V_ν denotes the electrostatic potential acting on atom ν. $(\partial Q_\nu/\partial V_{\nu'})$ can be evaluated by the second derivative of the energy with respect to the electrostatic potentials acting on atoms ν and ν' [for details, see Eq. (7) in Ref. 10].

B. Solvent-polarizable RISM theory for neat solvent systems

In a neat solvent, a polarized charge on a solvent atom is independent of its position because the system is homogeneous and has translational invariance. The polarized charge can thus be given by[18]

$$\Delta Q_\nu^0 = \sum_{\nu'} K_{\nu\nu'}\rho_{\nu'} \int_0^\infty \frac{Q_{\nu'}^0}{r} g_{\nu\nu'}(r) 4\pi r^2 dr, \tag{4}$$

where ρ_ν and $g_{\nu\nu'}(r)$ denote the number density of solvent atom ν and the radial distribution function (RDF) between atoms ν and ν', respectively. $Q_\nu^0 = Q_\nu^{\mathrm{vac}} + \Delta Q_\nu^0$ is the partial charge of the solvent after electronic polarization. In the RISM frame, the RDFs are obtained by solving the RISM equation for a neat solvent system,

$$\boldsymbol{h} = \boldsymbol{\omega} * \boldsymbol{c} * \boldsymbol{\omega} + \boldsymbol{\omega} * \boldsymbol{c} * \boldsymbol{\rho}\boldsymbol{h}, \tag{5}$$

coupled with a closure equation, such as the Kovalenko–Hirata (KH) closure,

$$g_{\nu\nu'}(r) = \begin{cases} \exp\{d_{\nu\nu'}(r)\}, & d_{\nu\nu'}(r) > 0 \\ d_{\nu\nu'}(r) + 1, & d_{\nu\nu'}(r) \le 0, \end{cases} \tag{6}$$

$$d_{\nu\nu'}(r) = -\beta u_{\nu\nu'}(r) + h_{\nu\nu'}(r) - c_{\nu\nu'}(r), \tag{7}$$

where $\boldsymbol{h}$, $\boldsymbol{c}$, $\boldsymbol{\omega}$, and $\boldsymbol{\rho}$ are the matrices having the elements $h_{\nu\nu'}(r)$, $c_{\nu\nu'}(r)$, $\omega_{\nu\nu'}(r)$, and $\rho_\nu\delta_{\nu\nu'}$, respectively. $h_{\nu\nu'}(r)$, $c_{\nu\nu'}(r)$, and $\omega_{\nu\nu'}(r)$ denote the total, direct, and intramolecular correlation functions between the solvent sites ν and ν', respectively. The total correlation function is related to the RDF by $h_{\nu\nu'}(r) = g_{\nu\nu'}(r) - 1$. The asterisk in Eq. (5), "$*$," indicates the convolution integral, and $\beta = 1/k_{\mathrm{B}}T$ is the inverse temperature; $u_{\nu\nu'}$ is the intermolecular interaction potential given by

$$u_{\nu\nu'}(r) = u_{\nu\nu'}^{\mathrm{LJ}}(r) + u_{\nu\nu'}^{\mathrm{ES}}(r), \tag{8}$$

$$u_{\nu\nu'}^{\mathrm{LJ}}(r) = 4\epsilon_{\nu\nu'}\left\{\left(\frac{\sigma_{\nu\nu'}}{r}\right)^{12} - \left(\frac{\sigma_{\nu\nu'}}{r}\right)^{6}\right\}, \tag{9}$$

$$u_{\nu\nu'}^{\mathrm{ES}}(r) = \frac{Q_\nu^0 Q_{\nu'}^0}{r}, \tag{10}$$

where $\epsilon_{\nu\nu'}$ and $\sigma_{\nu\nu'}$ are the Lennard-Jones parameters with their usual meanings.

C. Solvent-polarizable 3D-RISM theory

Here, we consider the system in which a solute molecule of infinite dilution is immersed in the solvent. Unlike a neat solvent system, solvent-polarized charges depend on the position of the solvent site because the heterogeneous electrostatic potential due to the solute and solvent molecules affects the solvent polarization. The solvent-polarized charge density (PCD), $\rho_\nu g_\nu(\boldsymbol{r})\delta\Delta Q_\nu(\boldsymbol{r})$, around the solute molecule is then given as

$$\rho_\nu g_\nu(\boldsymbol{r})\delta\Delta Q_\nu(\boldsymbol{r}) = \sum_{\nu'} K_{\nu\nu'} \int \left\langle \rho_\nu(\boldsymbol{r})\rho_{\nu'}(\boldsymbol{r}')\right\rangle_{\mathrm{s}} V(\boldsymbol{r}')d\boldsymbol{r}', \tag{11}$$

where $\delta\Delta Q_\nu(\boldsymbol{r})$ is the change in polarized charge from that of the neat solvent, Q_ν^0. $g_\nu(\boldsymbol{r})$ is a special distribution function of solvent ν, which is obtained by solving the solute–solvent 3D-RISM equation

$$h_\nu(\boldsymbol{r}) = \sum_{\nu'} \int c_{\nu'}(\boldsymbol{r}')\left(\omega_{\nu'\nu}(\boldsymbol{r} - \boldsymbol{r}') + \rho_{\nu'} h_{\nu'\nu}(\boldsymbol{r} - \boldsymbol{r}')\right)d\boldsymbol{r}', \tag{12}$$

coupled with a closure equation such as the KH closure

$$g_\nu(\boldsymbol{r}) = \begin{cases} \exp\{d_\nu(\boldsymbol{r})\}, & d_\nu(\boldsymbol{r}) > 0 \\ d_\nu(\boldsymbol{r}) + 1, & d_\nu(\boldsymbol{r}) \le 0, \end{cases} \tag{13}$$

$$d_\nu(\boldsymbol{r}) = -\beta u_\nu^{\mathrm{CRK}}(\boldsymbol{r}) + h_\nu(\boldsymbol{r}) - c_\nu(\boldsymbol{r}). \tag{14}$$

Here, $u_\nu^{\mathrm{CRK}}(\boldsymbol{r})$ is the solute–solvent interaction potential function including the solvent-polarized charge. Equation (11) gives the PCD as a function of the electrostatic potential. There are four physical requirements that should be satisfied by this function as follows: (i) no polarized charge appears where no solvent is present, (ii) the electrostatic potential at a position with no solvent does not affect the PCD, (iii) the polarized charge should be conserved after being integrated over the whole space, and (iv) the application of a uniform electrostatic potential does not induce the charge polarization. The intramolecular density–density correlation function, denoted as $\langle \rho_\nu(\boldsymbol{r})\rho_{\nu'}(\boldsymbol{r})\rangle_{\mathrm{s}}$, should be handled in a proper way to fulfill all of these four requirements. Therefore, $\langle \rho_\nu(\boldsymbol{r})\rho_{\nu'}(\boldsymbol{r})\rangle_{\mathrm{s}}$ was evaluated in this study as the functional derivative of $g_\nu^{\mathrm{u}}(\boldsymbol{r})$ with respect to $u_\nu(\boldsymbol{r})$,

$$\left\langle \rho_\nu(\boldsymbol{r})\rho_{\nu'}(\boldsymbol{r}')\right\rangle_{\mathrm{s}} = -\frac{\rho_\nu \delta g_\nu^{\mathrm{u}}(\boldsymbol{r})}{\beta \delta u_{\nu'}(\boldsymbol{r}')}, \tag{15}$$

as was proposed by Yamaguchi *et al.*[27,28] In the functional derivative, a solvent molecule under consideration should be treated as "a solute" of infinite dilution to obtain the intramolecular correlation. $g_\nu^{\mathrm{u}}(\boldsymbol{r})$ is a special distribution function of solvent ν, which is obtained by solving the solute–solute 3D-RISM equation.[29] The detail of the solute–solute 3D-RISM equation is mentioned in Subsection II D.

In the present study, we examined four different schemes for treating the terms $V(\boldsymbol{r})$ and $u_\nu^{\mathrm{CRK}}(\boldsymbol{r})$. In Scheme I, only the electrostatic potential due to the solvent molecules was considered, so the electrostatic potential is given by

$$V(\boldsymbol{r}) = \sum_u \frac{q_u}{|\boldsymbol{r} - \boldsymbol{r}_u|} \equiv V_{\mathrm{solu}}(\boldsymbol{r}), \tag{16}$$

where q_u and $\boldsymbol{r}_u$ denote the point charge and the position of solute atom u, respectively. The corresponding interaction potential is

$$u_\nu^{\mathrm{CRK}}(\boldsymbol{r}) = u_\nu(\boldsymbol{r}) + \frac{1}{2}\delta\Delta Q_\nu(\boldsymbol{r}) V_{\mathrm{solu}}(\boldsymbol{r}), \tag{17}$$

where

$$u_\nu(\boldsymbol{r}) = Q_\nu^0 V_{\mathrm{solu}}(\boldsymbol{r}) + \sum_u \left[4\epsilon_{u\nu} \left\{ \left(\frac{\sigma_{u\nu}}{|\boldsymbol{r} - \boldsymbol{r}_u|} \right)^{12} - \left(\frac{\sigma_{u\nu}}{|\boldsymbol{r} - \boldsymbol{r}_u|} \right)^{6} \right\} \right]. \tag{18}$$

In this scheme, the electrostatic potential by other solvent molecules is ignored for $V(\boldsymbol{r})$. The second term on the right-hand side (rhs) of Eq. (17) corresponds to $-(\boldsymbol{\mu}\cdot\boldsymbol{E})/2$ of the classical electrodynamics, where $\boldsymbol{\mu}$ and $\boldsymbol{E}$ denote the induced dipole and electric field, respectively.[30] This scheme is similar to that by Naka *et al.*[18]

In Scheme II, the electrostatic potential produced by the static charges of other solvent molecules is included,

$$\begin{aligned} V(\boldsymbol{r}) &= V_{\mathrm{solu}}(\boldsymbol{r}) + \sum_{\nu'} \int \rho_{\nu'} g_{\nu'}(\boldsymbol{r}') \frac{Q_{\nu'}^0}{|\boldsymbol{r} - \boldsymbol{r}'|} \mathrm{erf}\left(\alpha|\boldsymbol{r} - \boldsymbol{r}'|\right) d\boldsymbol{r}' \\ &= V_{\mathrm{solu}}(\boldsymbol{r}) + V_{\mathrm{solv}}^{\mathrm{stat}}(\boldsymbol{r}), \end{aligned} \tag{19}$$

where the error function was introduced to remove the self-interaction and α is an adjustable damping factor. In addition to Scheme II, the electrostatic potential by the polarized solvent charge induced by a solute molecule is also considered in Scheme III,

$$\begin{aligned} V(\boldsymbol{r}) &= V_{\mathrm{solu}}(\boldsymbol{r}) + V_{\mathrm{solv}}^{\mathrm{stat}}(\boldsymbol{r}) \\ &\quad + \sum_{\nu'} \int \rho_{\nu'} g_{\nu'}(\boldsymbol{r}') \frac{\delta\Delta Q_{\nu'}(\boldsymbol{r}')}{|\boldsymbol{r} - \boldsymbol{r}'|} \mathrm{erf}\left(\alpha|\boldsymbol{r} - \boldsymbol{r}'|\right) d\boldsymbol{r}' \\ &= V_{\mathrm{solu}}(\boldsymbol{r}) + V_{\mathrm{solv}}^{\mathrm{stat}}(\boldsymbol{r}) + V_{\mathrm{solv}}^{\mathrm{pol}}(\boldsymbol{r}). \end{aligned} \tag{20}$$

For Schemes II and III, the interaction potential, $u_\nu^{\mathrm{CRK}}(\boldsymbol{r})$, is the same as that of Scheme I. In these schemes, $g_\nu(\boldsymbol{r})$, the distribution of solvent molecules, does not reflect the changes in the electrostatic potential due to $\delta\Delta Q_\nu(\boldsymbol{r})$. To consider such an effect, we employed the following interaction potential in Scheme IV:

$$\begin{aligned} u_\nu^{\mathrm{CRK}}(\boldsymbol{r}) &= u_\nu(\boldsymbol{r}) + \frac{1}{2}\delta\Delta Q_\nu(\boldsymbol{r}) \left(V_{\mathrm{solu}}(\boldsymbol{r}) + V_{\mathrm{solv}}^{\mathrm{stat}}(\boldsymbol{r}) + V_{\mathrm{solv}}^{\mathrm{pol}}(\boldsymbol{r}) \right) \\ &\quad + Q_\nu^0 V_{\mathrm{solv}}^{\mathrm{pol}}(\boldsymbol{r}). \end{aligned} \tag{21}$$

Because $u_\nu^{\mathrm{CRK}}(\boldsymbol{r})$ includes $\delta\Delta Q_\nu(\boldsymbol{r})$ in both Eqs. (17) and (21), the 3D-RISM/KH equation and Eq. (11) are iteratively solved to obtain the self-consistent solution.

The renormalized solute–solvent interactions, $u_\nu^{\mathrm{CRK}}(\boldsymbol{r})$ in Eqs. (17) and (21), are given an *ansatz* in this subsection, and their derivations using a density functional formalism will be given in Sec. II E for Schemes I and IV.

We refer to the 3D-RISM taking solvent polarization into account with CRK as the sp-3D-RISM theory. For discrimination, the conventional 3D-RISM theory without a solvent polarization model is called the nonpolarizable 3D-RISM (np-3D-RISM).

D. Intramolecular density–density correlation function

In this subsection, a method for the numerical computation of the intramolecular density–density correlation function, Eq. (15), is proposed. To consider the functional derivative in Eq. (15), we introduce the interaction potential with a set of perturbation parameters, $\{\lambda_\nu\}$,

$$u_\nu^{(\lambda)}(\boldsymbol{r}) = u_\nu^0(\boldsymbol{r}) + \lambda_\nu V(\boldsymbol{r}). \tag{22}$$

Then, the corresponding distribution function, $g_\nu^{(\lambda)}(\boldsymbol{r})$, satisfies the relation as

$$\int \frac{\delta g_\nu^{(\lambda)}(\boldsymbol{r})}{\delta u_{\nu'}(\boldsymbol{r}')} V(\boldsymbol{r}') d\boldsymbol{r}' = \frac{\partial g_\nu^{(\lambda)}(\boldsymbol{r})}{\partial \lambda_{\nu'}}. \tag{23}$$

Using this equation, the following relation can be obtained:

$$-\sum_{\nu'} K_{\nu\nu'} \int \frac{\rho_\nu \delta g_\nu(\boldsymbol{r})}{\beta \delta u_{\nu'}(\boldsymbol{r}')} V(\boldsymbol{r}') d\boldsymbol{r}' = -\frac{\rho_\nu}{\beta} \sum_{\nu'} K_{\nu\nu'} \frac{\partial g_\nu^{(\lambda)}(\boldsymbol{r})}{\partial \lambda_{\nu'}}. \tag{24}$$

Combined with Eqs. (15) and (24), we finally obtain

$$\rho_\nu g_\nu(\boldsymbol{r}) \delta\Delta Q_\nu(\boldsymbol{r}) = -\frac{\rho_\nu}{\beta} \sum_{\nu'} K_{\nu\nu'} \frac{\partial g_\nu^{(\lambda)}(\boldsymbol{r})}{\partial \lambda_{\nu'}} = -\frac{\rho_\nu}{\beta} \frac{\partial g_\nu(\boldsymbol{r})}{\partial \gamma_\nu}. \tag{25}$$

In the last term, we omitted the superscript (λ) from $g_\nu(\boldsymbol{r})$ for simplicity, and we introduced a new coupling parameter, γ_ν, defined as

$$\lambda_{\nu'} = \sum_{\nu} K_{\nu\nu'}\gamma_\nu. \tag{26}$$

The derivative of the distribution function with respect to the perturbation parameter, $\partial g_\nu(\boldsymbol{r})/\partial\gamma_\nu$, is obtained by solving the coupled perturbed solute–solute 3D-RISM with the KH closure (CP-uu-3D-RISM/KH) equation as follows:

$$\frac{\partial g^{\mathrm{u}}_\nu(\boldsymbol{r})}{\partial\gamma_{\nu'}} = \begin{cases} \left(-\frac{\beta\partial u^{\mathrm{u}}_\nu(\boldsymbol{r})}{\partial\gamma_{\nu'}} + \frac{\partial g^{\mathrm{u}}_\nu(\boldsymbol{r})}{\partial\gamma_{\nu'}} - \frac{\partial c^{\mathrm{u}}_\nu(\boldsymbol{r})}{\partial\gamma_{\nu'}}\right) g^{\mathrm{u}}_\nu(\boldsymbol{r}) & \text{for} \quad g^{\mathrm{u}}_\nu(\boldsymbol{r}) < 1 \\ -\frac{\beta\partial u^{\mathrm{u}}_\nu(\boldsymbol{r})}{\partial\gamma_{\nu'}} + \frac{\partial g^{\mathrm{u}}_\nu(\boldsymbol{r})}{\partial\gamma_{\nu'}} - \frac{\partial c^{\mathrm{u}}_\nu(\boldsymbol{r})}{\partial\gamma_{\nu'}} & \text{for} \quad g^{\mathrm{u}}_\nu(\boldsymbol{r}) \geq 1, \end{cases} \tag{27}$$

$$\frac{\partial g^{\mathrm{u}}_\nu(\boldsymbol{r})}{\partial\gamma_{\nu'}} = \sum_{\nu''}\int \frac{\partial c^{\mathrm{u}}_{\nu''}(\boldsymbol{r}'')}{\partial\gamma_{\nu'}}\omega^{\mathrm{uu}}_{\nu''\nu}(|\boldsymbol{r}-\boldsymbol{r}''|)d\boldsymbol{r}''. \tag{28}$$

Here, one of the solvent molecules is regarded as "solute" to distinguish it from other solvents.[29] From Eqs. (22) and (26),

$$\frac{\partial u^{\mathrm{u}}_\nu(\boldsymbol{r})}{\partial\gamma_{\nu'}} = V(\boldsymbol{r})\frac{\partial\sum_{\nu''}K_{\nu\nu''}\gamma_{\nu''}}{\partial\gamma_{\nu'}} = K_{\nu\nu'}V(\boldsymbol{r}). \tag{29}$$

Defining $G_{\nu\nu'}(\boldsymbol{r}) = \partial g^{\mathrm{u}}_\nu(\boldsymbol{r})/\partial\gamma_{\nu'}$ and $C_{\nu\nu'}(\boldsymbol{r}) = \partial c^{\mathrm{u}}_\nu(\boldsymbol{r})/\partial\gamma_{\nu'}$ and introducing $T_{\nu\nu'}(\boldsymbol{r}) = G_{\nu\nu'}(\boldsymbol{r}) - C_{\nu\nu'}(\boldsymbol{r})$, Eqs. (27) and (28) become

$$C_{\nu\nu'}(\boldsymbol{r}) = \begin{cases} -\beta K_{\nu\nu'}V(\boldsymbol{r})g^{\mathrm{u}}_\nu(\boldsymbol{r}) + (g^{\mathrm{u}}_\nu(\boldsymbol{r})-1)T_{\nu\nu'}(\boldsymbol{r}) & \text{for } g^{\mathrm{u}}_\nu(\boldsymbol{r}) < 1 \\ -\beta K_{\nu\nu'}V(\boldsymbol{r}) & \text{for } g^{\mathrm{u}}_\nu(\boldsymbol{r}) \geq 1, \end{cases} \tag{30}$$

$$\tilde{T}_{\nu\nu'}(\boldsymbol{k}) = -\tilde{C}_{\nu\nu'}(\boldsymbol{k}) + \sum_{\nu''}\tilde{C}_{\nu''\nu'}(\boldsymbol{k})\tilde{\omega}^{\mathrm{uu}}_{\nu''\nu}(|\boldsymbol{k}|), \tag{31}$$

where $\tilde{T}_{\nu\nu'}(\boldsymbol{k})$ and $\tilde{C}_{\nu\nu'}(\boldsymbol{k})$ are the Fourier transforms of $T_{\nu\nu'}(\boldsymbol{r})$ and $C_{\nu\nu'}(\boldsymbol{r})$, respectively. Here, $V(\boldsymbol{r})$, $g^{\mathrm{u}}_\nu(\boldsymbol{r})$, and $\tilde{\omega}^{\mathrm{uu}}_{\nu\nu'}(|\boldsymbol{k}|)$ are given by the former calculations; hence, Eqs. (30) and (31) can be solved in an iterative manner to obtain

$$\rho_\nu g_\nu(\boldsymbol{r})\delta\Delta Q_\nu(\boldsymbol{r}) = \begin{cases} \frac{\rho_\nu g_\nu(\boldsymbol{r})}{\beta}\{\beta K_{\nu\nu}V(\boldsymbol{r}) - T_{\nu\nu}(\boldsymbol{r})\} & \text{for} \quad g^{\mathrm{u}}_\nu(\boldsymbol{r}) < 1 \\ \frac{\rho_\nu}{\beta}\{\beta K_{\nu\nu}V(\boldsymbol{r}) - T_{\nu\nu}(\boldsymbol{r})\} & \text{for} \quad g^{\mathrm{u}}_\nu(\boldsymbol{r}) \geq 1. \end{cases} \tag{32}$$

A similar relation can be obtained for the hypernetted-chain (HNC) closure instead of KH (see the supplementary material).

E. Free energy functional formalization of the sp-3D-RISM theory

In this subsection, we propose a free energy functional formalization of the sp-3D-RISM theory with Scheme IV. First, we overview the ordinary free energy functional formalism without electronic polarization.[31–33] The free energy of the system Ω_0 is described as a function of the solvent distribution function $g_\nu(\boldsymbol{r})$ in the absence of solute molecules, where the partial charge of the solvent, $Q^0_\nu = Q^{\mathrm{vac}}_\nu + \Delta Q^0_\nu$, is assumed to be independent of the electrostatic potential. The solvent distribution in the presence of solute molecules is obtained as that minimizing $\Omega_0[\{g_\nu(\boldsymbol{r})\}] + \sum_\nu \rho_\nu \int u_\nu(\boldsymbol{r})g_\nu(\boldsymbol{r})d\boldsymbol{r}$; therefore, it satisfies the relation

$$\rho_\nu u_\nu(\boldsymbol{r}) + \frac{\delta\Omega_0}{\delta g_\nu(\boldsymbol{r})} = 0, \tag{33}$$

which describes the conventional 3D-RISM equation without the electronic polarization of the solvent.

When the solvent charges polarize in response to the electrostatic potential, the total free energy of the system is extended as a functional of $g_\nu(\boldsymbol{r})$ and $\delta\Delta Q_\nu(\boldsymbol{r})$ by

$$\begin{aligned}\Omega_{\mathrm{tot}}[\{g_\nu(\boldsymbol{r}),\delta\Delta Q_\nu(\boldsymbol{r})\}] = {}& \Omega_0[\{g_\nu(\boldsymbol{r})\}] + \Omega_{\mathrm{pol}}[\{g_\nu(\boldsymbol{r}),\delta\Delta Q_\nu(\boldsymbol{r})\}] \\ & + \sum_\nu \rho_\nu \int u_\nu(\boldsymbol{r})g_\nu(\boldsymbol{r})d\boldsymbol{r} \\ & + \sum_\nu \rho_\nu \int V_{\mathrm{solu}}(\boldsymbol{r})\delta\Delta Q_\nu(\boldsymbol{r})g_\nu(\boldsymbol{r})d\boldsymbol{r},\end{aligned} \tag{34}$$

where $u_\nu(\boldsymbol{r})$ is a potential function given by Eq. (18); $g_\nu(\boldsymbol{r})$ and $\delta\Delta Q_\nu(\boldsymbol{r})$ are determined by minimizing Ω_{tot}, and these conditions lead to

$$\rho_\nu V_{\mathrm{solu}}(\boldsymbol{r})g_\nu(\boldsymbol{r}) + \frac{\delta\Omega_{\mathrm{pol}}}{\delta\Delta Q_\nu(\boldsymbol{r})} = 0, \tag{35}$$

$$\rho_\nu u_\nu(\boldsymbol{r}) + \rho_\nu V_{\mathrm{solu}}(\boldsymbol{r})\delta\Delta Q_\nu(\boldsymbol{r}) + \frac{\delta\Omega_0}{\delta g_\nu(\boldsymbol{r})} + \frac{\delta\Omega_{\mathrm{pol}}}{\delta g_\nu(\boldsymbol{r})} = 0. \tag{36}$$

From the comparison between Eqs. (33) and (36), Eq. (36) is equivalent to the 3D-RISM equation with the interaction potential

$$u^{\mathrm{CRK}}_\nu(\boldsymbol{r}) = u_\nu(\boldsymbol{r}) + V_{\mathrm{solu}}(\boldsymbol{r})\delta\Delta Q_\nu(\boldsymbol{r}) + \frac{1}{\rho_\nu}\frac{\delta\Omega_{\mathrm{pol}}}{\delta g_\nu(\boldsymbol{r})}, \tag{37}$$

instead of $u_\nu(\boldsymbol{r})$.

The solvent polarization term of the free energy functional, Ω_{pol}, is given by

$$\begin{aligned}\Omega_{\mathrm{pol}}[\{g_\nu(\boldsymbol{r}),\delta\Delta Q_\nu(\boldsymbol{r})\}] = {}& \sum_{\nu\nu'}\iint \rho_\nu h_\nu(\boldsymbol{r})Q^0_\nu W(\boldsymbol{r},\boldsymbol{r}')\rho_{\nu'}g_{\nu'}(\boldsymbol{r}')\delta\Delta Q_{\nu'}(\boldsymbol{r}')d\boldsymbol{r}d\boldsymbol{r}' \\ & + \frac{1}{2}\sum_{\nu\nu'}\iint \rho_\nu g_\nu(\boldsymbol{r})\delta\Delta Q_\nu(\boldsymbol{r})W(\boldsymbol{r},\boldsymbol{r}')\rho_{\nu'}g_{\nu'}(\boldsymbol{r}')\delta\Delta Q_{\nu'}(\boldsymbol{r}')d\boldsymbol{r}d\boldsymbol{r}' \\ & - \frac{1}{2}\sum_{\nu\nu'}\iint \rho_\nu g_\nu(\boldsymbol{r})\delta\Delta Q_\nu(\boldsymbol{r})M^{-1}_{\nu\nu'}(\boldsymbol{r},\boldsymbol{r}')\rho_{\nu'}g_{\nu'}(\boldsymbol{r}')\delta\Delta Q_{\nu'}(\boldsymbol{r}')d\boldsymbol{r}d\boldsymbol{r}',\end{aligned} \tag{38}$$

where

$$W(\boldsymbol{r},\boldsymbol{r}') = \frac{\mathrm{erf}(\alpha|\boldsymbol{r}-\boldsymbol{r}'|)}{|\boldsymbol{r}-\boldsymbol{r}'|}, \tag{39}$$

$$M_{\nu\nu'}(\boldsymbol{r},\boldsymbol{r}') = K_{\nu\nu'}\langle\rho_\nu(\boldsymbol{r})\rho_{\nu'}(\boldsymbol{r}')\rangle_{\mathrm{s}}. \tag{40}$$

The physical meanings of Eq. (38) are as follows. The first term describes the electrostatic interaction energy between the fixed and polarized charges of the solvents, and the second term is that between polarized charges of different solvent molecules. The last term stands for the energy cost to distort the intramolecular electronic state of the solvent. Substitution of Eq. (38) into Eq. (35) leads to

$$\begin{aligned}
&\rho_\nu g_\nu(\boldsymbol{r})\delta\Delta Q_\nu(\boldsymbol{r}) \\
&= \sum_{\nu'\nu''}\iint M_{\nu\nu'}(\boldsymbol{r},\boldsymbol{r}')W(\boldsymbol{r}',\boldsymbol{r}'')h_{\nu''}(\boldsymbol{r}'')\rho_{\nu''}Q^0_{\nu''}d\boldsymbol{r}''d\boldsymbol{r}' \\
&\quad + \sum_{\nu'\nu''}\iint M_{\nu\nu'}(\boldsymbol{r},\boldsymbol{r}')W(\boldsymbol{r}',\boldsymbol{r}'')g_{\nu''}(\boldsymbol{r}'')\rho_{\nu''}\delta\Delta Q_{\nu''}(\boldsymbol{r}'')d\boldsymbol{r}''d\boldsymbol{r}' \\
&\quad + \sum_{\nu'}\int M_{\nu\nu'}(\boldsymbol{r},\boldsymbol{r}')V_{\mathrm{solu}}(\boldsymbol{r}')d\boldsymbol{r}' \\
&= \sum_{\nu'}\int M_{\nu\nu'}(\boldsymbol{r},\boldsymbol{r}')V(\boldsymbol{r}')d\boldsymbol{r}',
\end{aligned} \tag{41}$$

where

$$V(\boldsymbol{r}) = V_{\mathrm{solu}}(\boldsymbol{r}) + V^{\mathrm{stat}}_{\mathrm{solv}}(\boldsymbol{r}) + V^{\mathrm{pol}}_{\mathrm{solv}}(\boldsymbol{r}). \tag{42}$$

Equation (41) with Eq. (42) is equivalent to Eq. (11) combined with Eq. (20) in Scheme IV.

The solute–solvent interaction potential with solvent charge polarization, $u^{\mathrm{CRK}}_\nu(\boldsymbol{r})$ of Eq. (21), is derived by substituting Eq. (38) into Eq. (37) as

$$\begin{aligned}
u^{\mathrm{CRK}}_\nu(\boldsymbol{r}) &= u_\nu(\boldsymbol{r}) + Q^0_\nu\sum_{\nu'}\int W(\boldsymbol{r},\boldsymbol{r}')\rho_{\nu'}g_{\nu'}(\boldsymbol{r}')\delta\Delta Q_{\nu'}(\boldsymbol{r}')d\boldsymbol{r}' \\
&\quad - \frac{1}{2\rho_\nu}\sum_{\nu'\nu''}\iint \rho_{\nu'}g_{\nu'}\delta\Delta Q_{\nu'}(\boldsymbol{r}') \\
&\quad \times \frac{\delta M^{-1}_{\nu'\nu''}}{\delta g_\nu(\boldsymbol{r})}\rho_{\nu''}g_{\nu''}(\boldsymbol{r}'')\delta\Delta Q_{\nu''}(\boldsymbol{r}'')d\boldsymbol{r}''d\boldsymbol{r}'.
\end{aligned} \tag{43}$$

The second term on the rhs of Eq. (43) can be rewritten as

$$Q^0_\nu\sum_{\nu'}\int W(\boldsymbol{r},\boldsymbol{r}')\rho_{\nu'}g_{\nu'}(\boldsymbol{r}')\delta\Delta Q_{\nu'}(\boldsymbol{r}')d\boldsymbol{r}' = Q^0_\nu V^{\mathrm{pol}}_{\mathrm{solu}}(\boldsymbol{r}), \tag{44}$$

and the third term is

$$\begin{aligned}
&-\frac{1}{2\rho_\nu}\sum_{\nu'\nu''}\iint \rho_{\nu'}g_{\nu'}\delta\Delta Q_{\nu'}(\boldsymbol{r}') \\
&\times \frac{\delta M^{-1}_{\nu'\nu''}(\boldsymbol{r}',\boldsymbol{r}'')}{\delta g_\nu(\boldsymbol{r})}\rho_{\nu''}g_{\nu''}(\boldsymbol{r}'')\delta\Delta Q_{\nu''}(\boldsymbol{r}'')d\boldsymbol{r}''d\boldsymbol{r}' \\
&= \frac{1}{2\rho_\nu}\sum_{\nu'\nu''}\iint V(\boldsymbol{r}')\frac{\delta M_{\nu'\nu''}(\boldsymbol{r}',\boldsymbol{r}'')}{\delta g_\nu(\boldsymbol{r})}V(\boldsymbol{r}'')d\boldsymbol{r}''d\boldsymbol{r}' \\
&\approx \frac{1}{2}V(\boldsymbol{r})\delta\Delta Q_\nu(\boldsymbol{r}).
\end{aligned} \tag{45}$$

The details of the approximation applied for the last part are given in the supplementary material. Substituting Eqs. (44) and (45) into Eq. (43) gives

$$u^{\mathrm{CRK}}_\nu(\boldsymbol{r}) = u_\nu(\boldsymbol{r}) + Q^0_\nu V^{\mathrm{pol}}_{\mathrm{solu}}(\boldsymbol{r}) + \frac{1}{2}V(\boldsymbol{r})\delta\Delta Q_\nu(\boldsymbol{r}), \tag{46}$$

which corresponds to Eq. (21).

Scheme I can also be derived in the free energy functional formalism. In this case, Ω_{pol} in Eq. (38) is replaced as

$$\begin{aligned}
\Omega_{\mathrm{pol}}[\{g_\nu(\boldsymbol{r}),\delta\Delta Q_\nu(\boldsymbol{r})\}] &= -\frac{1}{2}\sum_{\nu\nu'}\iint \rho_\nu g_\nu(\boldsymbol{r})\delta\Delta Q_\nu(\boldsymbol{r})M^{-1}_{\nu\nu'}(\boldsymbol{r},\boldsymbol{r}') \\
&\quad \times \rho_{\nu'}g_{\nu'}(\boldsymbol{r}')\delta\Delta Q_{\nu'}(\boldsymbol{r}')d\boldsymbol{r}d\boldsymbol{r}'.
\end{aligned} \tag{47}$$

Comparing Eqs. (41) and (47), it is clear that the electrostatic interaction of a polarized charge on a solvent with other solvents is neglected in Scheme I.

F. Analytical expression of solvation free energy for sp-3D-RISM theory

The solvation free energy is given by the Kirkwood charging formula as

$$\Delta\mu = \sum_\nu\rho_\nu\int_0^1 d\lambda\left[\frac{du_\nu(\boldsymbol{r})}{d\lambda}g_\nu(\boldsymbol{r}) + \frac{dV_{\mathrm{solu}}(\boldsymbol{r})}{d\lambda}g_\nu(\boldsymbol{r})\delta\Delta Q_\nu(\boldsymbol{r})\right], \tag{48}$$

where λ is the charging parameter. Using Eqs. (35) and (36), the solvation free energy can be rewritten as

$$\begin{aligned}
\Delta\mu &= \Omega_0[\{g_\nu(\boldsymbol{r})\}] + \Omega_{\mathrm{pol}}[\{g_\nu(\boldsymbol{r}),\delta\Delta Q_\nu(\boldsymbol{r})\}] \\
&\quad + \sum_\nu\rho_\nu\int u_\nu(\boldsymbol{r})g_\nu(\boldsymbol{r})d\boldsymbol{r} \\
&\quad + \sum_\nu\rho_\nu\int V_{\mathrm{solu}}(\boldsymbol{r})g_\nu(\boldsymbol{r})\delta\Delta Q_\nu(\boldsymbol{r})d\boldsymbol{r}.
\end{aligned} \tag{49}$$

Because $g_\nu(\boldsymbol{r})$, the distribution function, is determined by solving the 3D-RISM equation, the Singer–Chandler formula for the solvation free energy, $\Delta\mu_{\mathrm{SC}}$, is related to $\Omega_0[\{g_\nu(\boldsymbol{r})\}]$ as

$$\Delta\mu_{\mathrm{SC}} = \Omega_0[\{g_\nu(\boldsymbol{r})\}] + \sum_\nu\rho_\nu\int u^{\mathrm{CRK}}_\nu(\boldsymbol{r})g_\nu(\boldsymbol{r})d\boldsymbol{r}. \tag{50}$$

Substituting Eqs. (38) and (50) into Eq. (49), an analytical expression of solvation free energy for the sp-3D-RISM theory with Scheme IV can be obtained as

$$\begin{aligned}
\Delta\mu &= \Delta\mu_{\mathrm{SC}} + \Omega_{\mathrm{pol}}[\{g_\nu(\boldsymbol{r}),\delta\Delta Q_\nu(\boldsymbol{r})\}] \\
&\quad - \sum_\nu\rho_\nu\int\left[u^{\mathrm{CRK}}_\nu(\boldsymbol{r}) - u_\nu(\boldsymbol{r})\right]g_\nu(\boldsymbol{r})d\boldsymbol{r} \\
&\quad + \sum_\nu\rho_\nu\int V_{\mathrm{solu}}(\boldsymbol{r})g_\nu(\boldsymbol{r})\delta\Delta Q_\nu(\boldsymbol{r})d\boldsymbol{r} \\
&= \Delta\mu_{\mathrm{sc}} - \sum_\nu\rho_\nu\int g_\nu(\boldsymbol{r})\left(Q^0_\nu + \frac{1}{2}\delta\Delta Q_\nu(\boldsymbol{r})\right)V^{\mathrm{pol}}_{\mathrm{solv}}(\boldsymbol{r})d\boldsymbol{r}.
\end{aligned} \tag{51}$$

In the case of Scheme I, the use of Eq. (47) instead of Eq. (41) gives the simple expression for the solvation free energy as

$$\Delta\mu = \Delta\mu_{SC}. \tag{52}$$

III. COMPUTATIONAL DETAILS

In the present study, we examine the water solvent at 298.0 K with a number density of 0.0334 Å^{-3}. The Lennard-Jones parameter for the solvent water is taken from the simple point charge (SPC) model with a modified hydrogen parameter σ_H = 1.00 Å and ϵ_H = 0.046 kcal/mol.[34,35] The CRK and the molecular structure of the solvent water are taken from the literature.[10] The point charge of the solvent water *in vacuo* is determined by the electrostatic potential method with the restricted Hartree–Fock/double zeta plus polarization (RHF/DZP) level. The dielectric constant for the dielectric-consistent RISM (DRISM) calculation is set at 78.5.[36] The dielectric correction of sp-3D-RISM is described in detail in Sec. IV B. The number of grid points for the computation of the neat solvent system is 2048 with a grid width of 0.05 Å. We also used the SPC/E model[34] for comparison. The adjustable damping factor α in Eq. (19) was set to 0.5 Å^{-1}. Other values of α are examined in the supplementary material.

For the solute–solvent system, we examined ions and small molecules as solute molecules, namely, Na^+, K^+, Cl^-, I^-, Ca^{2+}, acetone, and alanine. The optimized potentials for liquid simulations (OPLS) for all atoms (-AA) and the united atom (-UA) and the generalized Amber force field (GAFF) parameter were used for ions, acetone, and alanine, respectively.[37–41] The molecular structure of alanine was determined by RHF/DZP with a polarizable continuum model calculation. The number of grid points for the 3D-RISM calculation was 128^3 with a grid width of 0.25 Å for a monatomic solute and 0.5 Å for molecules.

All the calculations were conducted using the RISM integrated calculator (RISMiCal) program package developed by us.[42–44]

IV. RESULTS AND DISCUSSION

A. Neat solvent system

The solvent distribution and the charge polarization of the neat solvent system were examined. In Table I, the point charges on the solvent water in the neat solvent are summarized. By applying the solvent-polarizable model, the polarization of the solvent water was drastically enhanced. The point charge on the oxygen atom was negatively enhanced as ΔQ_v^0 = −0.2738 and −0.2693 for standard RISM and DRISM, respectively. The standard RISM provided the dielectric constant ε = 32.4, whereas that of DRISM was set to 78.5. In the case of DRISM, the polarization was slightly smaller than for standard RISM.

In Fig. 1, the RDFs of water are depicted, and the results are compared for solvent-polarizable (sp)-DRISM, nonpolarizable (np)-DRISM), and DRISM with the SPC/E model. The np-DRISM calculations used $\{Q_v^{vac}\}$ for the solvent point charges. For both oxygen–oxygen of water (O_w–O_w) and oxygen–hydrogen of water (O_w–H_w), the RDFs of np-DRISM and DRISM/SPCE show similar behavior despite the differences in charge. By contrast, the RDF of sp-DRISM shows significant differences. The second peak of O_w–O_w RDF of sp-DRISM appears at 4.6 Å, which is called the *finger-print peak*,

TABLE I. Point charge on the solvent water in the neat solvent.

	Point charge			
Atom	Q_v^{vac}	Q_v^0(sp-RISM)	Q_v^0 (sp-DRISM)	SPC/E
O	−0.806	−1.0798	−1.0753	−0.8476
H	0.403	0.5399	0.5376	0.4238

whereas np-DRISM and DRISM/SPCE have no peaks in this region. The third peak is at 5.7 Å, which is very close to the second peaks of np-DRISM and DRISM/SPCE. The O_w–O_w RDF of SPC/E water with σ_H = 1.00 Å by RISM theory is known to have no finger-print peak because of the approximations inherent in the RISM theory.[21] In the case of O_w–H_w RDF, the first and second peaks of sp-DRISM were higher than those of np-DRISM and DRISM/SPC, but their positions are almost the same. These features indicate that the charge polarization enhanced the hydrogen-bond network in the neat solvent system.

For all subsequent analyses, the DRISM was used for computing the solvent–solvent correlation functions.

B. Dielectric behavior

The solvent polarization strongly affects the dielectric behavior, which is important for considering the electrostatic solvation in the polar solvent. In this subsection, we examine the dielectric behavior of the sp-3D-RISM theory in the long-range continuum limit.

The dielectric constant in the optical frequency limit is related to the refractive index, n, by $\varepsilon_\infty = n^2$, corresponding to the dielectric constant when the solvent density field remains in its equilibrium without the applied field, while the polarization charge responds fully to the applied field. The dielectric constant at zero frequency limit is evaluated under the condition that both the solvent density field and the polarization charge density relax to the equilibrium values under the applied field. The analytical expressions of the dielectric constant at both zero and optical frequencies based on the sp-3D-RISM theory with different approximation schemes are summarized in Table II. In this study, we assumed that a periodic electrostatic potential is applied to a homogeneous liquid. The dielectric constant was obtained from the long-wavelength limit of the charge density as the linear response of the electrostatic potential. The dielectric constant of the np scheme, ε_{np}, is related to the low-q behavior of the charge density fluctuation as[13]

$$\left(1 - \frac{1}{\varepsilon_{np}}\right) = \lim_{\boldsymbol{q}\to\boldsymbol{0}} \frac{4\pi\beta}{q^2} \sum_{v,v'} Q_v\left[\rho_v \tilde{\omega}_{vv'}(\boldsymbol{q}) + \rho_v \tilde{h}_{vv'}(\boldsymbol{q})\rho_{v'}\right]Q_{v'}. \tag{53}$$

Because the dielectric correction methods for the RISM theory, such as DRISM or the dielectric-consistent Stell correction,[45] are corrections for the charge density fluctuation in the long-wavelength limit, they can be used for the present theory "as is," so long as Eq. (53) is satisfied. The details of the derivation of these expressions are given in the supplementary material. Here, ε_∞ and ε denote the dielectric constant of optical and zero frequency limits, respectively. In the present study, ε_{np} was set at 78.5 for the DRISM calculations. Thus,

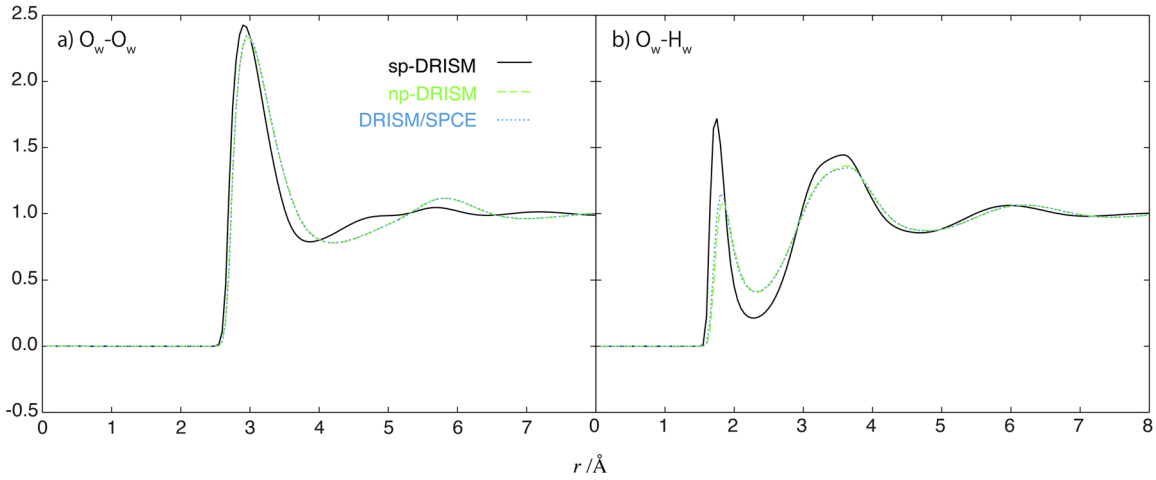

FIG. 1. RDFs of the solvent water between (a) oxygen atoms of water (O_w–O_w) and (b) oxygen and hydrogen atoms of water (O_w–H_w). Black solid, green dashed, and cyan dotted lines denote the results by sp-DRISM, np-DRISM, and DRISM with SPC/E water parameters, respectively.

the value of ε is different from the value used as the input parameter of the DRISM calculation. ρ_v and α_v are the number density and polarizability of the solvent, respectively. The polarizability of a solvent molecule can be related to CRK as

$$\alpha_v = -\frac{1}{3}\sum_{vv'} K_{vv'}(\boldsymbol{r}_v \cdot \boldsymbol{r}_{v'}). \tag{54}$$

In Table II, Schemes I and II have the same expression of ε_∞, whereas Schemes III and IV have another one. In Fig. 2, ε_∞ is plotted against the polarizability density, $4\pi\rho_v\alpha_v$, and is compared with the Lorentz–Lorenz relation,[30]

$$\frac{\varepsilon_\infty - 1}{\varepsilon_\infty + 2} = 4\pi\rho_v\alpha_v. \tag{55}$$

None of the four schemes can reproduce the Lorentz–Lorenz relation. The partial loss of information on the orientational correlation in the interaction-site model might be responsible for the deviation from the Lorentz–Lorenz relation. Schemes III and IV behave quantitatively better than Schemes I and II because the latter pair quickly diverge with an increasing polarizability density, whereas the former pair are linear. The ε_∞ values of all these schemes are smaller than the experimental one (≈1.78). This underestimation may originate from a lack of out-of-plane polarization of water in the present model.

The functional form of ε for Scheme I in Table II suggests the possibility of a nonphysical divergence in the case of strongly polar and polarizable solvents. Actually, the ε value in Scheme I becomes negative in the present case. Although finite, for Schemes II and III, the ε value can be unphysically large in the presence of electronic polarization. The ε values of Schemes II and III are 105.37 and 98.52, respectively, which are much larger than the dielectric constant of the neat solvent, 78.5. In contrast, Scheme IV has a physically reasonable expression because the electronic and nuclear

TABLE II. Expression for the dielectric constant for each scheme. The numbers in parentheses are the computed values with the present solvent model.

	Scheme			
	I	II	III	IV
ε_∞	$\frac{1}{1-4\pi\rho_v\alpha_v}$ (1.34)	$\frac{1}{1-4\pi\rho_v\alpha_v}$ (1.34)	$4\pi\rho_v\alpha_v + 1$ (1.25)	$4\pi\rho_v\alpha_v + 1$ (1.25)
ε	$\frac{\varepsilon_\infty\varepsilon_{np}}{\varepsilon_\infty+\varepsilon_{np}-\varepsilon_\infty\varepsilon_{np}}$ (−4.13)	$\varepsilon_\infty\varepsilon_{np}$ (105.37)	$\varepsilon_\infty\varepsilon_{np}$ (98.52)	$\varepsilon_\infty+\varepsilon_{np}+1$ (78.75)

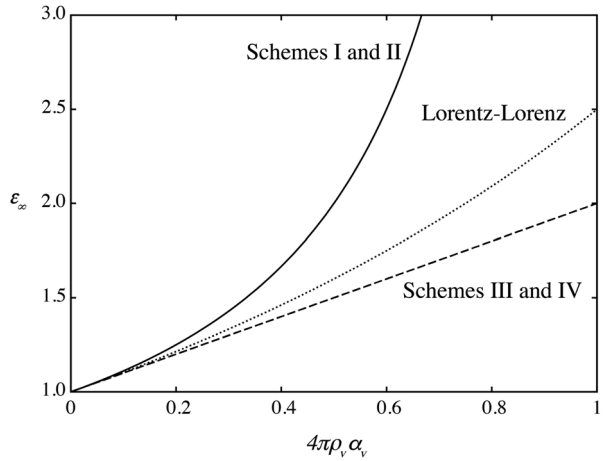

FIG. 2. Dielectric behavior in different schemes. Solid, dashed, and dotted lines depict Schemes I and II, Schemes III and IV, and the Lorentz–Lorenz relation, respectively.

polarizations are additive, and ε takes a reasonable value, 78.75. Therefore, we conclude that Scheme IV shows the best dielectric behavior among the four schemes, and Scheme IV was used for further analysis.

C. Solvent polarization around monatomic ions

The solvent polarization induced by simple monatomic ions is examined in this subsection. The PCD distributions and the

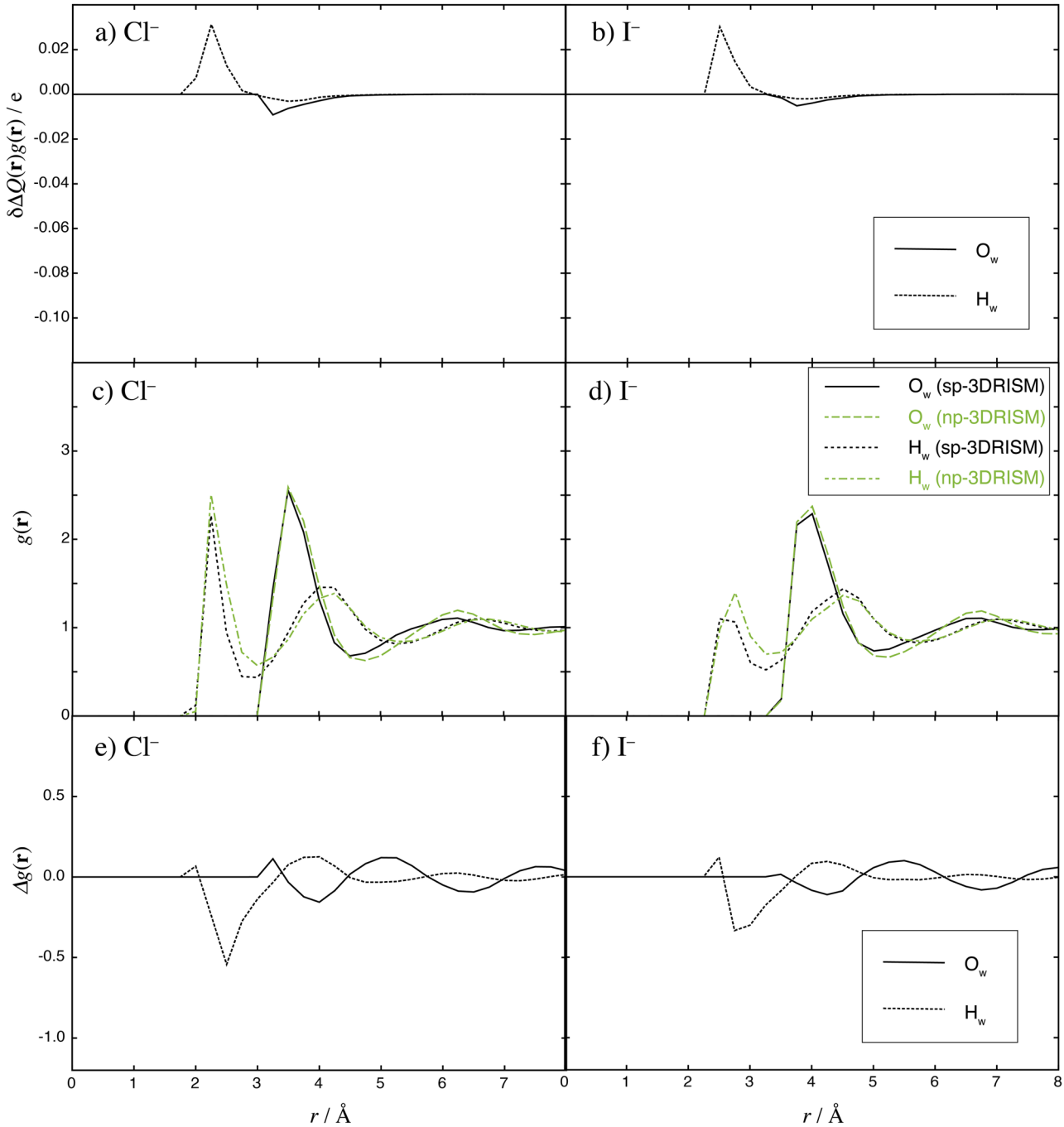

FIG. 3. Polarized charge densities around the (a) chloride and (b) iodide ions, the RDFs around the (c) chloride and (d) iodide ions, and the $\Delta g(r)$ around the (e) chloride and (f) iodide ions. Solid and dotted lines denote the oxygen and hydrogen atoms of the solvent computed by sp-3D-RISM, respectively; green dashed and dashed–dotted lines denote oxygen and hydrogen by np-3D-RISM, respectively.

RDFs around the anions are depicted in Fig. 3. Because one of the positively charged H_w atoms in the first solvation shell orients to an anion, the first RDF peak of hydrogen appears at around 2.5 Å, and the PCD of hydrogen shows a positive peak at the position. By contrast, a negative peak of the PCD of oxygen appeared at 3.6 Å, which corresponds to the first RDF peak. The hydrogen atom near the second RDF peak, which corresponds to another H_w atom in the first solvation shell, has weak negative polarization. In the case of the iodide ion, although the peak positions of both the PCD and the RDF shift to a long range, they behave similarly to the chloride ion case.

The results for the cations are depicted in Fig. 4. The negatively charged O_w atom of the solvent water was oriented to the solute cation; therefore, the first RDF peak of oxygen appears closer than that of the positively charged hydrogen atom. According to this picture, the polarization of an oxygen atom near a solute cation becomes negative, and hence, that of the hydrogen atom connecting to the oxygen becomes positive.

In the case of the sodium ion, the O_w atom of the solvent water is negatively polarized at contact distance from the ion. The polarization rapidly decays away from the ion because the electric field of the ion is screened by solvating water molecules. At the short-range side of the second RDF peak, the oxygen shows positive polarization, which may be induced by the negatively polarized oxygen at the first solvation shell. The hydrogen also shows negative polarization near the first RDF peak. This unexpected negative peak of hydrogen may be attributed to the orientational fluctuation of the water molecule. When one of the hydrogen atoms oriented to the opposite side of a cation has a large positive polarization, the other hydrogen atom can have negative polarization. Actually, the PCD of hydrogen has a positive value at the long-range side of the first peaks of hydrogen RDF. These polarizations of the solvent water cause the RDF peaks to be lower than those of the np-3D-RISM results; in addition, the peak positions are slightly shifted to the shorter range. Because the peak height is determined by the competition between the ion–water and the water–water interactions, it is considered that in this case,

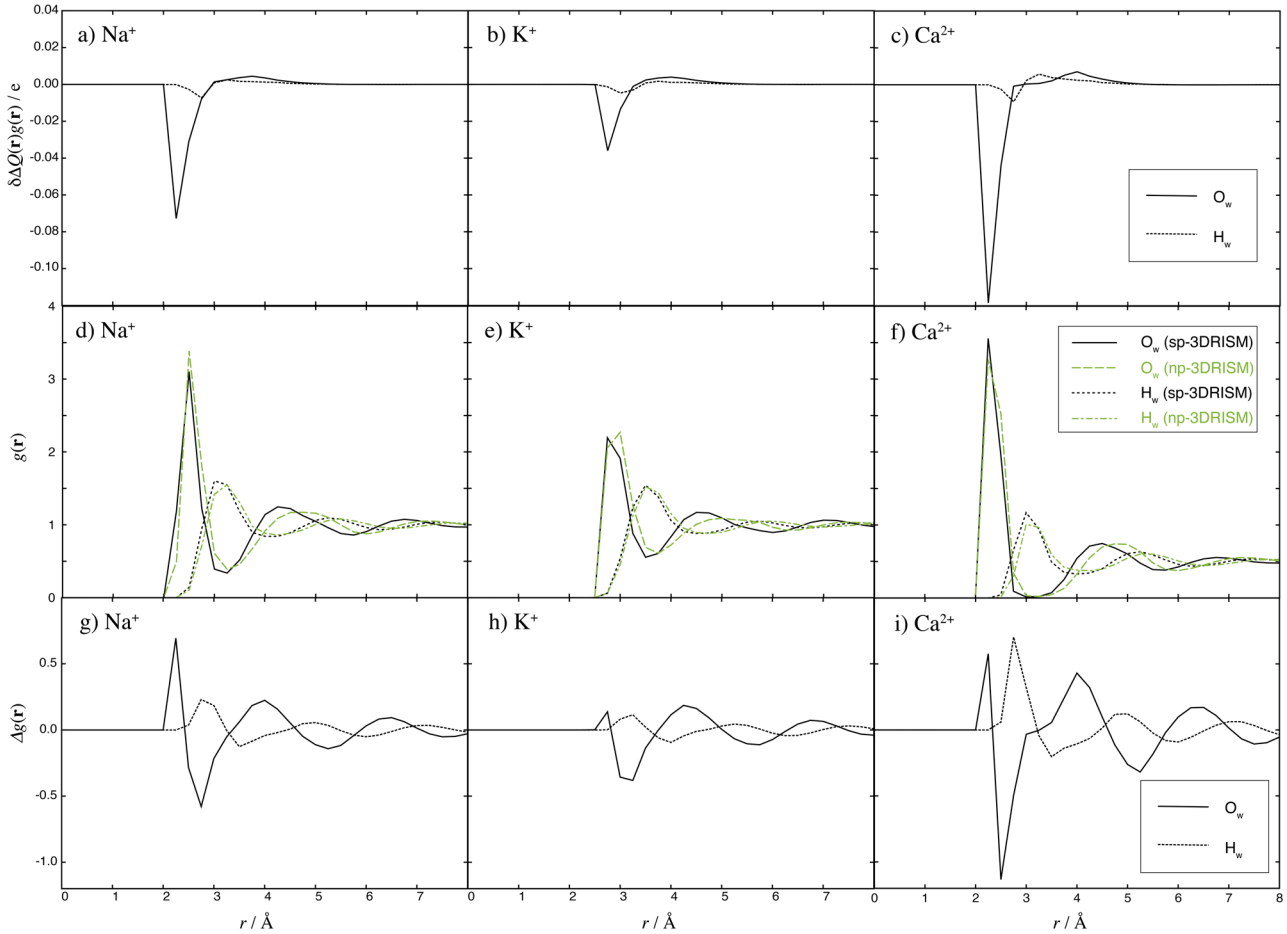

FIG. 4. Polarized charge densities around the (a) sodium, (b) potassium, and (c) calcium ions, the RDFs around the (d) sodium, (e) potassium, and (f) calcium ions, and the $\Delta g(r)$ around the (g) sodium, (h) potassium, and (i) calcium ions. Solid and dotted lines denote the oxygen and hydrogen atoms of the solvent computed by sp-3D-RISM, respectively; green dashed and dashed–dotted lines are oxygen and hydrogen by np-3D-RISM, respectively.

the peak was reduced due to the enhancement of the water–water interaction due to the polarization. A potassium ion shows a similar tendency to that of the sodium ion, although the peak height is smaller, and the position is shifted to the longer range due to the larger ionic radius of the potassium ion. A calcium ion shows a similar, but more enhanced, behavior compared with the monovalent cations. The polarization of the solvent around the calcium ion was much larger than that around the sodium and potassium ions.

The effect of introducing the solvent-polarizable model on the solvation free energy was also examined. In Table III, the solvation free energies evaluated by sp- and np-3D-RISM are summarized. As shown in Figs. 3 and 4, the solvent water molecules were polarized in response to the electric field by the solute ions. Therefore, the ions were stabilized with the polarizable rather than nonpolarizable solvent. In the present study, monovalent ions were more stabilized in the polarizable solvent by about 3–6 kcal mol^{-1}. The calcium ion, a divalent cation, shows a much stronger stabilization by polarization than the monovalent ions (−19.6 kcal mol^{-1}). These results suggest that the polarization of the solvent molecules has a strong effect on the solvation of the ions and that its magnitude significantly depends on the solute net charges.

D. Solvent polarization around polyatomic molecules

The effects of solvent polarization on the solvation of polar molecules, namely, acetone and alanine, were considered.

In Fig. 5, contour plots of PCD, $\delta\Delta Qg$, and the change in the distribution function, $\Delta g(\boldsymbol{r}) = g^{\mathrm{sp-3DRISM}}(\boldsymbol{r}) - g^{\mathrm{np-3DRISM}}(\boldsymbol{r})$, around solute acetone are shown. An acetone molecule has a dipole moment along the carbonyl C=O axis and the oxygen has a negative point charge. The H_w forming a hydrogen bond with the carbonyl oxygen has a positively polarized charge induced by the negatively charged carbonyl oxygen, and the O_w outside the positively polarized hydrogen distribution is negatively polarized. The distribution of H_w near the carbonyl oxygen increases, whereas the distribution just outside decreases. This means that the distribution of hydrogen shifts toward inside and the height decreases, which is similar to the monatomic anion cases. The PCD around the carbonyl oxygen shows a similar behavior to that around the anion. At the opposite side of carbonyl oxygen, close to the methyl group, both the solvent oxygen and the hydrogen are negatively polarized, and the oxygen, in particular, shows a stronger polarization than the hydrogen because the positive methyl groups are mainly solvated by the oxygen.

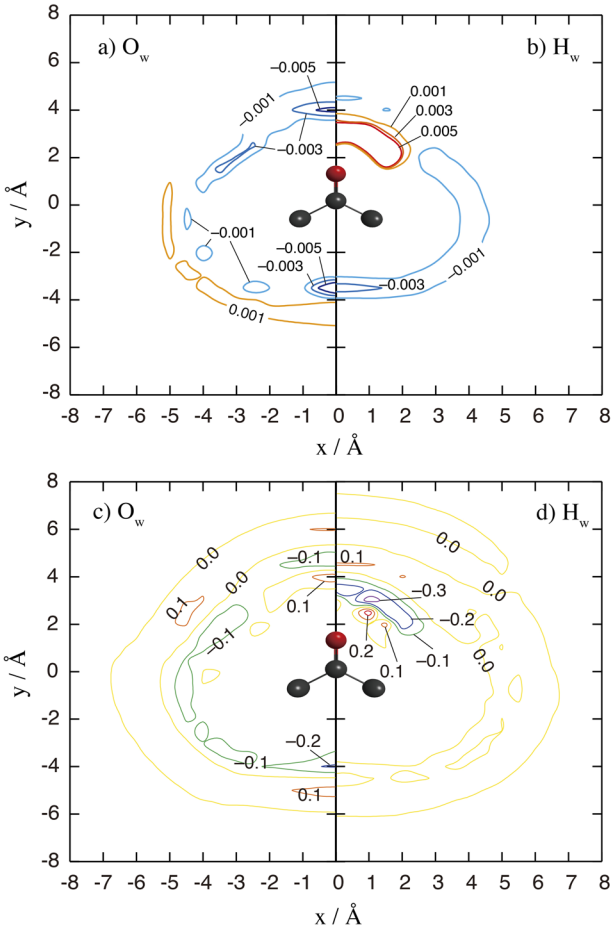

FIG. 5. (a) and (b) are the contour plots of polarized charge density, $\delta\Delta Q(\boldsymbol{r})g(\boldsymbol{r})$, and (c) and (d) are the relative spatial distribution functions, $\Delta g(\boldsymbol{r})$, around solute acetone. (a) and (c) are those of O_w, whereas (b) and (d) are those of H_w.

TABLE III. Solvation free energies of the ions and molecules. Units are given in kcal mol^{-1}. Numbers in parentheses are relative values from np-3D-RISM.

Solute	$\Delta\mu$ (sp-3D-RISM)		$\Delta\mu$ (np-3D-RISM)
Na^+	−77.2	(−3.8)	−73.4
K^+	−57.0	(−2.8)	−54.2
Cl^-	−89.1	(−6.1)	−83.0
I^-	−70.0	(−5.7)	−64.3
Ca^{2+}	−358.6	(−19.6)	−339.0
Acetone	8.2	(−2.7)	10.9
Alanine	−34.5	(−6.8)	−27.7

An alanine molecule was also considered as an example of polar solute molecules, which takes a zwitterionic form, where the carboxyl and amine groups have negative and positive net charges, respectively. In addition, alanine has a hydrophobic methyl group. In Fig. 6, spatial distributions of PCD, $\delta\Delta Qg$, are depicted. The solvent oxygen was negatively polarized around the positively charged amine group, while the solvent hydrogen was positively polarized around the negatively charged carboxyl group. Such behavior corresponds to the polarization around monatomic ions described above. In contrast, neither oxygen nor hydrogen showed noticeable polarization around the hydrophobic methyl group. The changes in the distributions of oxygen and hydrogen, Δg, are depicted in Figs. 7(a) and 7(b), respectively. The distributions of oxygen and hydrogen were enhanced around the amine and carboxyl groups, and decreased just outside of them. These behaviors correspond to the cases of cation and anion, respectively.

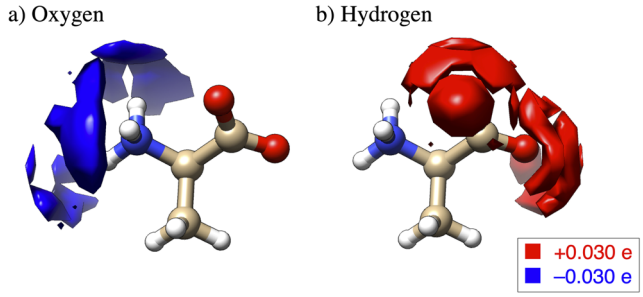

FIG. 6. Spatial distributions of polarized charge density, $\delta\Delta Q(\boldsymbol{r})g(\boldsymbol{r})$, of (a) O_w and (b) H_w of the solvent water around the alanine zwitterion. Red and blue surfaces are isosurfaces $\delta\Delta Q(\boldsymbol{r})g(\boldsymbol{r})$ = +0.03e and −0.03e, respectively.

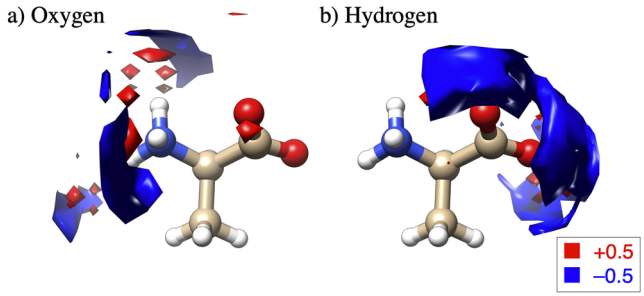

FIG. 7. Relative spatial distributions, $\Delta g(\boldsymbol{r})$, of (a) O_w and (b) H_w of the solvent water around the alanine zwitterion. Red and blue surfaces are isosurfaces $\Delta g(\boldsymbol{r})$ = +0.5 and −0.5, respectively.

The solvation free energies of acetone and alanine are presented in Table III. Similar to the ions, the solvent polarization stabilizes them. The alanine showed a stronger stabilization than acetone. Owing to its larger partial charges, the alanine induces a higher polarization on the solvent molecule, resulting in stronger stabilization.

V. SUMMARY

We proposed the sp-3D-RISM theory, which takes the charge polarization of solvent molecules into account using the CRK method. Four different coupling schemes were considered. Among these, Scheme IV showed a reasonable dielectric behavior because it has no divergent character and presents additivity for electronic and orientational polarizations, and numerical relevance compared with the Lorentz–Lorenz relation. Scheme IV considers the effect of both the solute and solvent molecules including the electronic polarization of the solvent. The sp-3D-RISM was also formalized based on the free energy functional, and the analytical expression for the solvation free energy was derived.

The sp-3D-RISM theory with Scheme IV was applied to the solvation of the monatomic ions and polar polyatomic molecules in water. The solvent water molecules were polarized around the solute molecules according to the electrostatic potential by both the solute and solvent molecules: namely, the oxygen atom oriented toward the cations or the positively charged atoms was negatively charged, and the hydrogen atom forming a hydrogen bond to the anions or the negatively charged atoms was positively charged. In addition, the polarized solvent molecules near the solute affected the polarization of other solvent molecules. We also examined the effect of the solvent polarization on the solvation free energy. For all the solute molecules, the solvation free energy became lower due to the polarization, in particular, the divalent calcium cation showed a strong stabilization.

The numerical results indicated that the solvent molecules near the polar solutes showed significant polarization, and hence, the model proposed here is useful for considering the solvation process and the thermodynamics of polar solute molecules, such as electron transfer reactions in solutions or biological systems. Furthermore, the method proposed here can be combined with a quantum chemical electronic structure theory in solution such as 3D-RISM-SCF.[24,46] The combination of the 3D-RISM-SCF with sp-3D-RISM allows us to examine the solute electronic structure including the excited state in detail, which is applicable, for example, to the photo-induced excited state electron transfer reaction in solution. Such studies are currently in progress in our group.

SUPPLEMENTARY MATERIAL

See the supplementary material for the derivation and data that support the findings of this study and the derivation of the sp-3D-RISM with HNC closure, details of approximation in Eq. (45), the derivation of dielectric constants, assessment of the damping factor, spatial distribution around polyatomic molecules, and force field parameters.

ACKNOWLEDGMENTS

We are grateful for the financial support from JSPS KAKENHI (Grant No. 19H02677). N.Y. acknowledges the Toyota Riken Scholar from Toyota Physical and Chemical Research Institute. Numerical calculations were conducted in part at the Research Center for Computational Science, Institute for Molecular Science, National Institutes of Natural Sciences. Molecular graphics were depicted with UCSF Chimera, developed by the Resource for Biocomputing, Visualization, and Informatics at the University of California, San Francisco.[47]

REFERENCES

[1] O. M. Becker, A. D. MacKerell, Jr., B. Roux, and M. Watanabe, *Computational Biochemistry and Biophysics* (Mercel Dekker, New York, 2001).
[2] L. X. Dang, J. Chem. Phys. **97**, 2659–2660 (1992).
[3] J. Brodholt, M. Sampoli, and R. Vallauri, Mol. Phys. **86**, 149–158 (1995).
[4] I. M. Svishchev, P. G. Kusalik, J. Wang, and R. J. Boyd, J. Chem. Phys. **105**, 4742–4750 (1996).
[5] A. Morita and S. Kato, J. Am. Chem. Soc. **119**, 4021–4032 (1997).
[6] P. J. van Maaren and D. van der Spoel, J. Phys. Chem. B **105**, 2618–2626 (2001).
[7] H. A. Stern, F. Rittner, B. J. Berne, and R. A. Friesner, J. Chem. Phys. **115**, 2237–2251 (2001).
[8] H. Yu, T. Hansson, and W. F. van Gunsteren, J. Chem. Phys. **118**, 221–234 (2003).
[9] G. Lamoureux, A. D. MacKerell, Jr., and B. Roux, J. Chem. Phys. **119**, 5185–5197 (2003).
[10] A. Morita and S. Kato, J. Chem. Phys. **108**, 6809–6818 (1998).

[11] S. Iuchi, A. Morita, and S. Kato, J. Phys. Chem. B **106**, 3466–3476 (2002).
[12] T. Ishiyama and A. Morita, J. Phys. Chem. C **111**, 738–748 (2007).
[13] T. Ishiyama and A. Morita, J. Phys. Chem. C **111**, 721–737 (2007).
[14] T. Ishiyama and A. Morita, J. Phys. Chem. A **111**, 9277–9285 (2007).
[15] T. Ishiyama and A. Morita, J. Chem. Phys. **131**, 244714 (2009).
[16] T. Ishiyama and A. Morita, J. Phys. Chem. C **113**, 16299–16302 (2009).
[17] R. Kusaka, T. Ishiyama, S. Nihonyanagi, A. Morita, and T. Tahara, Phys. Chem. Chem. Phys. **20**, 3002–3009 (2018).
[18] K. Naka, A. Morita, and S. Kato, J. Chem. Phys. **111**, 481–491 (1999).
[19] D. Chandler and H. C. Andersen, J. Chem. Phys. **57**, 1930–1937 (1972).
[20] F. Hirata and P. Rossky, Chem. Phys. Lett. **83**, 329–334 (1981).
[21] F. Hirata, *Molecular Theory of Solvation* (Kluwer, Dordrecht, 2003).
[22] D. Beglov and B. Roux, J. Phys. Chem. B **101**, 7821–7826 (1997).
[23] A. Kovalenko and F. Hirata, Chem. Phys. Lett. **290**, 237–244 (1998).
[24] A. Kovalenko and F. Hirata, J. Chem. Phys. **110**, 10095–10112 (1999).
[25] N. Yoshida, T. Imai, S. Phongphanphanee, A. Kovalenko, and F. Hirata, J. Phys. Chem. B **113**, 873–886 (2009).
[26] N. Yoshida, J. Chem. Inf. Model. **57**, 2646–2656 (2017).
[27] T. Yamaguchi, T. Matsuoka, and S. Koda, J. Chem. Phys. **123**, 034504 (2005).
[28] K. Kasahara and H. Sato, J. Chem. Phys. **145**, 194502 (2016).
[29] Y. Kiyota, N. Yoshida, and F. Hirata, J. Chem. Theory Comput. **7**, 3803–3815 (2011).
[30] J. D. Jackson, *Classical Electrodynamics*, 3rd ed. (Wiley, New York, NY, 1999).
[31] D. Chandler, J. D. Mccoy, and S. J. Singer, J. Chem. Phys. **85**, 5971–5976 (1986).
[32] D. Chandler, J. D. Mccoy, and S. J. Singer, J. Chem. Phys. **85**, 5977–5982 (1986).
[33] J. P. Hansen and I. R. McDonald, *Theory of Simple Liquids*, 3rd ed. (Academic Press, Amsterdam, 2006).
[34] M. R. Reddy and M. Berkowitz, Chem. Phys. Lett. **155**, 173–176 (1989).
[35] S. Ten-no, F. Hirata, and S. Kato, J. Chem. Phys. **100**, 7443–7453 (1994).
[36] J. Perkyns and B. M. Pettitt, Chem. Phys. Lett. **190**, 626–630 (1992).
[37] J. Chandrasekhar, D. C. Spellmeyer, and W. L. Jorgensen, J. Am. Chem. Soc. **106**, 903–910 (1984).
[38] S. Weiner, P. Kollman, D. Case, U. Singh, C. Ghio, G. Alagona, S. Profeta, and P. Weiner, J. Am. Chem. Soc. **106**, 765–784 (1984).
[39] J. Aqvist, J. Phys. Chem. **94**, 8021–8024 (1990).
[40] J. M. Wang, R. M. Wolf, J. W. Caldwell, P. A. Kollman, and D. A. Case, J. Comput. Chem. **25**, 1157–1174 (2004).
[41] J. Wang, W. Wang, P. A. Kollman, and D. A. Case, J. Mol. Graphics Modell. **25**, 247–260 (2006).
[42] N. Yoshida and F. Hirata, J. Comput. Chem. **27**, 453–462 (2006).
[43] N. Yoshida, J. Chem. Phys. **140**, 214118 (2014).
[44] The details of the RISMiCal package is in https://sites.google.com/site/norioyoshida1973/rismical.
[45] T. Yamaguchi and S. Koda, Bull. Chem. Soc. Jpn. **88**, 804–813 (2015).
[46] H. Sato, A. Kovalenko, and F. Hirata, J. Chem. Phys. **112**, 9463–9468 (2000).
[47] E. F. Pettersen, T. D. Goddard, C. C. Huang, G. S. Couch, D. M. Greenblatt, E. C. Meng, and T. E. Ferrin, J. Comput. Chem. **25**, 1605–1612 (2004).